Opportunistic Symbiotic Backscatter Communication Systems

Hancheng Yang, Haiyang Ding, *Member, IEEE*, and Maged Elkashlan, *Senior Member, IEEE*

***Abstract*— This letter proposes an opportunistic commensal mechanism (OppCom) and an opportunistic parasitic mechanism (OppPar) for a pair of backscatter devices (BDs) to strengthen the concurrent transmission of the primary and the backscatter systems. It is shown that the asymptotic outage probability of the OppCom and OppPar mechanisms is not affected by the channel statistics between the two BDs. Also, for the OppPar mechanism, the backscatter efficiency ratio between the two BDs, instead of their individual values, dominates the system outage performance and a larger difference of the backscatter efficiencies leads to a better transmission robustness.**

***Index Terms*— Symbiotic radio, backscatter communications, outage probability.**

I. Introduction

With the rapid rise of 5G era, Internet of Things (IoT) technology, as a new generation of communication technology, finds wide applications in the areas of social production, medical treatment, logistics, military and other aspects [1], [2]. Among many enabling techniques of IoT, backscatter communications have the advantage of low power consumption and high spectrum efficiency by employing the passive modulation nature in the RF domain.

In this regard, V. Liu *et al.* proposed an ambient backscatter communication (AmBC) system and designed a backscatter transceiver which can harvest RF energy, transmit and receive without the expensive process of generating radio waves [3]. Up to that time, backscatter communication can be classified into three major types, namely, monostatic backscatter communication (MBC), bistatic backscatter communications (BiBC), and AmBC [4].

Recently, a new idea, namely, the passive backscatter transmission that shares not only the same radio-frequency source but also the same spectrum with the active primary transmission, was put forward, which has the potential to achieve higher spectral and energy efficiencies [5]. Subsequently, in [6], a novel symbiotic radio paradigm was introduced and three practical spectrum sharing mechanisms, a.k.a., commensal, parasitic, and competitive schemes, were proposed. [7] investigated the outage probability of the aforementioned three backscatter communication mechanisms, and derived the corresponding asymptotic outage performance. *However, due to the impacts of obstacles, path loss, and wireless channel fading, the environmental electromagnetic (EM) signals are not stable and can be challenging to utilize. This opportunistic availability of the environmental EM signals calls for an opportunistic backscatter mechanism to strengthen the transmission robustness of the backscatter link. In addition, for such an opportunistic/adaptive backscatter transmitter-receiver setup, the reflection coefficient at BD and the transmit power at PT become very involved to determine, which leads to a more complicated outage analysis, as will be shown afterwards.*

In this letter, in order to make an adaptive symbiotic transmission of the primary and backscatter systems feasible, we propose an opportunistic commensal (OppCom) mechanism as well as an opportunistic parasitic (OppPar) mechanism. We then develop the optimal setup of reflection coefficient at the BD and the primary transmit power at the RF source for the two mechanisms, respectively. Our analysis shows that for both OppCom and OppPar, the high-SNR outage probability is not affected by the channel statistics between the pair of BDs. In addition, it is shown that unlike OppCom, the ratio of the backscatter efficiencies pertaining to the two BDs plays a critical role in the outage performance of the OppPar mechanism.

II. System Model and Protocol Designs

A. System Model

As shown in Fig. 1, we consider a backscatter communication system with two BDs (i.e., BD1 and BD2), which opportunistically transmit the signal $C_1(n)$ or $C_2(n)$ (BD1 transmits $C_1(n)$ to BD2, and BD2 transmits $C_2(n)$ to BD1) to each other with the aid of primary signal $S(n)$ as a carrier. Without loss of generality, it is assumed that the signals $S(n)$, $C_1(n)$, and $C_2(n)$ are normalized, and the primary transmitter and receiver are denoted as PT and PR, respectively.

To proceed, we denote the channel coefficients pertaining to the links from PT to PR, from PT to BD1, from PT to BD2, and from BD1 to BD2 as h_0, h_1, h_2 and h_{12}, respectively. Herein, the channel reciprocity is assumed such that $h_{12} = h_{21}$ [3]. Accordingly, d_0, d_1, d_2 and d_{12} are used to denote the distances of the corresponding links. Based on the Rayleigh fading assumptions,[1] we assume that $|h_0|^2 \sim \exp(\lambda_0^*)$, $|h_1|^2 \sim \exp(\lambda_1^*)$, $|h_2|^2 \sim \exp(\lambda_2^*)$ and $|h_{12}|^2 \sim \exp(\lambda_{12}^*)$, respectively. To incorporate the path loss effects, we use β to represent the path loss exponent, and attain that $\lambda_0^* = d_0^{-\beta}$, $\lambda_1^* = d_1^{-\beta}$, $\lambda_2^* = d_2^{-\beta}$ and $\lambda_{12}^* = d_{12}^{-\beta}$. To facilitate the subsequent representation, we define $\lambda_0 = 1/\lambda_0^*$, $\lambda_1 = 1/\lambda_1^*$, $\lambda_2 = 1/\lambda_2^*$, and $\lambda_{12} = 1/\lambda_{12}^*$. In addition, since PR is usually located far away from BD, the backscatter signal from BD to PR is insignificant and is ignored [6].

[1] It is important to note that unlike Rician channel assumption, Gaussian channel (i.e., Rayleigh fading) can better model the propagation environment with blockages and rich scattering paths, such as indoor/urban backscatter applications. In addition, Gaussian channel assumption is often employed to evaluate the worst/limiting performance of a given backscatter system.

Manuscript received 4 August 2022; revised 25 August 2022; accepted 25 August 2022. Date of publication 26 August 2022; date of current version 9 January 2023. This work was supported in part by the National Key R&D Program of China under Grant 2018YFE0100500, and in part by the National Natural Science Foundation of China under Grant 61871387. The associate editor coordinating the review of this letter and approving it for publication was M. Koca. *(Corresponding author: Haiyang Ding.)*

Hancheng Yang and Haiyang Ding are with the School of Information and Communications, National University of Defense Technology, Wuhan 430010, China, and also with the Youth Innovation Team of Shaanxi Universities, Shaanxi 710021, China (e-mail: dinghy2003@nudt.edu.cn).

Maged Elkashlan is with the School of Electronic Engineering and Computer Science, Queen Mary University of London, E1 4NS London, U.K. (e-mail: maged.elkashlan@qmul.ac.uk).

Digital Object Identifier 10.1109/LCOMM.2022.3202362

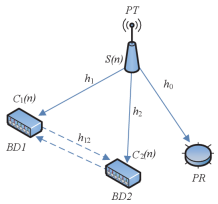

Fig. 1. System model.

As a result, the n-th received signal at PR can be written as $y_0(n) = \sqrt{P_s}h_0S(n) + U_0(n)$, where P_s denotes the transmit power at PT, $U_0(n)$ represents the normalized additive white Gaussian noise (AWGN) signal at PR with $E(|U_0(n)|^2) = 1$. Therefore, the received signal-to-noise ratio (SNR) of the primary link can be expressed as $\gamma_0 = P_s|h_0|^2$.

As aforementioned, BD1 or BD2 is opportunistically designated as the backscatter transmitter for each backscatter time slot, while the other backscatter device is determined as the backscatter receiver accordingly. The detailed decision rule will be introduced next. Therefore, if BD2 is designated as the backscatter transmitter, the received signal at BD1 can be expressed as

$$y_1(n) = \sqrt{P_s}h_1S(n) + \sqrt{P_s\alpha_2\eta_2}h_{12}h_2S(n)C_2(n) + U_1(n). \quad (1)$$

In contrast, if BD1 is designated as the backscatter transmitter, the received signal at BD2 can be written as $y_2(n) = \sqrt{P_s}h_2S(n) + \sqrt{P_s\alpha_1\eta_1}h_{12}h_1S(n)C_1(n) + U_2(n)$, where α_1 and α_2 represent the reflection coefficients of BD1 and BD2, whereas η_1 and η_2 denote the backscatter efficiencies of BD1 and BD2, respectively. In addition, $U_1(n)$ and $U_2(n)$ denote the normalized AWGN at BD1 and BD2, respectively.

For either of the above two cases, the successive interference cancellation (SIC) [8], [9] is implemented at the backscatter receiver such that $S(n)$ and $C_1(n)$ (or $C_2(n)$) are decoded successively. As a result, when decoding $S(n)$ from $y_1(n)$, the received signal-to-interference-and-noise ratio (SINR) at BD1 is given by

$$\gamma_1 = \frac{P_s|h_1|^2}{P_s\alpha_2\eta_2|h_2|^2|h_{12}|^2 + 1}. \quad (2)$$

If $S(n)$ can be successfully decoded from $y_1(n)$, the received SNR at BD1 to decode $C_2(n)$ can be expressed as

$$\gamma_{1c} = P_s\alpha_2\eta_2|h_2|^2|h_{12}|^2. \quad (3)$$

When decoding $S(n)$ from $y_2(n)$, the corresponding SINR at BD2 can be expressed as $\gamma_2 = \frac{P_s|h_2|^2}{P_s\alpha_1\eta_1|h_1|^2|h_{12}|^2+1}$.

Afterwards, if $S(n)$ is decoded successfully from $y_2(n)$, the received SNR at BD2 to decode $C_1(n)$ can be written as $\gamma_{2c} = P_s\alpha_1\eta_1|h_1|^2|h_{12}|^2$.

B. Protocol Design

1) Commensal Mechanism: In order to guarantee the concurrent transmission of both primary system and AmBC (or BiBC) system, the reflection coefficient α is adjusted such that the signal $S(n)$ from the primary system can be successfully decoded at the backscatter receiver based on the SIC rule. Specifically, when BD2 acts as the backscatter transmitter and BD1 acts as the backscatter receiver, the reflection coefficient of BD2 can be written as[2] $\alpha_2^* = \left[\min(1, \frac{|h_1|^2-|h_0|^2}{P_s\eta_2|h_0|^2|h_2|^2|h_{12}|^2})\right]^+$. On the contrary, when BD1 acts as the backscatter transmitter, the reflection coefficient of BD1 can be written as $\alpha_1^* = \left[\min(1, \frac{|h_2|^2-|h_0|^2}{P_s\eta_1|h_0|^2|h_1|^2|h_{12}|^2})\right]^+$.

To facilitate the protocol design, we define $MC_2 = \frac{|h_1|^2-|h_0|^2}{P_s\eta_2|h_0|^2|h_2|^2|h_{12}|^2}$, and $MC_1 = \frac{|h_2|^2-|h_0|^2}{P_s\eta_1|h_0|^2|h_1|^2|h_{12}|^2}$. Based on MC_1 and MC_2, the decision rule for the OppCom mechanism is shown in Table I such that the backscatter signal can be decoded more reliably at the receiver side.

2) Parasitic Mechanism: For the parasitic mechanism, which is applicable to the BiBC system, we set $\alpha = 1$ to maximize the backscatter channel capacity and then dynamically adjust the transmit power P_s at PT so that the backscatter receiver can successfully recover $C_1(n)$ (or $C_2(n)$). We refer to this procedure as an opportunistic parasitic (OppPar) mechanism. Specifically, when BD2 is designated as the backscatter transmitter and BD1 as the backscatter receiver, the SIC condition must be satisfied to guarantee the successful decoding of $S(n)$ such that the transmit power of PT should obey $P_{s1} = \left(\frac{|h_1|^2-|h_0|^2}{\eta_2|h_{12}|^2|h_0|^2|h_2|^2}\right)^+$. In contrast, if BD2 is designated as the backscatter receiver, we have $P_{s2} = \left(\frac{|h_2|^2-|h_0|^2}{\eta_1|h_{12}|^2|h_0|^2|h_1|^2}\right)^+$.

To facilitate the following discussion, we define $P_2 = \frac{|h_2|^2-|h_0|^2}{\eta_1|h_{12}|^2|h_0|^2|h_1|^2}$, $P_1 = \frac{|h_1|^2-|h_0|^2}{\eta_2|h_{12}|^2|h_0|^2|h_2|^2}$, and formulate the decision rule for the OppPar mechanism such that the backscatter signal can be recovered more reliably at the receiver side, as shown in Table I.

TABLE I
THE DECISION RULE FOR THE OPPCOM/OPPPAR MECHANISM

CSI conditions	Backscatter rule
Case 1: $\theta_1 < 0$, $\theta_2 < 0$	No backscatter transmission
Case 2: $\theta_1 < 0$, $\theta_2 > 0$	BD2 as Tx, BD1 as Rx
Case 3: $\theta_1 > 0$, $\theta_2 < 0$	BD1 as Tx, BD2 as Rx
Case 4-1: $\theta_1 > 0$, $\theta_2 > 0$,$\gamma_{1c} < \gamma_{2c}$	BD1 as Tx, BD2 as Rx
Case 4-2: $\theta_1 > 0$, $\theta_2 > 0$,$\gamma_{1c} > \gamma_{2c}$	BD2 as Tx, BD1 as Rx

[1] For OppCom, $\theta_1 = MC_1$ and $\theta_2 = MC_2$. For OppPar, $\theta_1 = P_1$ and $\theta_2 = P_2$.

III. OUTAGE ANALYSIS

A. OppCom Mechanism

In order to recover $C_1(n)$ (or $C_2(n)$) at the backscatter receiver, the received SNR to decode $C_2(n)$ (or $C_1(n)$) at BD1 (or BD2) has to satisfy $\gamma_{1c} > \tau_0$ (or $\gamma_{2c} > \tau_0$). Herein, τ_0 denotes the decoding threshold for $C_1(n)$ and $C_2(n)$. In what follows, we analyze the outage probability of the OppCom mechanism by examining the joint probabilities of each case listed in Table I.

[2]Note that the local channel state information (CSI) h_0 can be acquired at PT by estimating the pilot signal sent from PR, whereas the local CSI h_1 and h_2 at PT can be attained by estimating the round-trip backscatter channels PT-BD1-PT and PT-BD2-PT as in [10]. Next, these local CSI can be broadcast by PT and then obtained at BD1 and BD2. After which, PT transmits the pilot signal again such that BD2 (or BD1) can acquire its local CSI h_{12} by first estimating the cascaded backscatter channel PT-BD1-BD2 (or PT-BD2-BD1) and then attaining h_{12} by eliminating the known CSI h_1 (or h_2). Thus far, the global CSI is available at BD1 and BD2. Finally, BD1 can forward h_{12} to PT by remodulating the pilot signal from PT via the round-trip backscatter channel PT-BD1-PT. This way, the global CSI can also be attained at PT.

Case 1 ($MC_2 < 0$, $MC_1 < 0$): In this case, no matter how to schedule the backscatter transmitter and receiver, one cannot find a feasible setup of the reflection coefficient α, resulting in a backscatter transmission outage. To proceed, we define $Z \triangleq |h_0|^2$, $X \triangleq |h_1|^2$, $Y \triangleq |h_2|^2$ and $U \triangleq |h_{12}|^2$. Mathematically [11], we can formulate the probability of outage events as below

$$\begin{aligned} P_{out1}^{comm} &= \Pr(MC_1 < 0, MC_2 < 0) \\ &= 1 + \frac{\lambda_0}{\lambda_0+\lambda_1+\lambda_2} - \frac{\lambda_0}{\lambda_0+\lambda_2} - \frac{\lambda_0}{\lambda_0+\lambda_1}. \end{aligned} \quad (4)$$

Case 2 ($MC_2 > 0$, $MC_1 < 0$): In this case, only BD2 can be selected as the backscatter transmitter with a feasible reflection coefficient α. However, when $C_2(n)$ cannot be decoded at BD1, the backscatter transmission is bound to be interrupted, whose probability can be written as

$$\begin{aligned} P_{out2}^{comm} = &\Pr\left(0 < \frac{X-Z}{ZYU} < P_s\eta_2, \frac{Y}{Z} < 1, \frac{X-Z}{Z} < \tau_0\right) \\ &+ \Pr\left(\frac{X-Z}{ZYU} > P_s\eta_2, \frac{Y}{Z} < 1, YU < \frac{\tau_0}{P_s\eta_2}\right). \end{aligned} \quad (5)$$

To proceed, we first formulate the following lemmas.

Lemma 1: For independent random variables X, Y, and Z with arbitrary distributions, it follows that $\lim_{P\to\infty} \Pr(X < PY, X < Z) = \Pr(X < Z)$.

Proof: Please refer to Appendix A.

Lemma 2: For independent random variables X, Y, Z, and U with arbitrary distributions, it follows that $\lim\limits_{P\to\infty} \Pr(X > PY, U < Z) = 0$.

Proof: By following a similar procedure as in Appendix A, we can complete the proof.

With the aid of Lemmas 1 and 2, at high transmit SNR, (5) can be asymptotically written as

$$\begin{aligned} &\lim_{P\to\infty} P_{out2}^{comm} \\ &= \Pr\left(Y < Z, \frac{X-Z}{Z} < \tau_0\right) \\ &= \frac{\lambda_0}{\lambda_0+\lambda_1} - \frac{\lambda_0}{\lambda_0+\lambda_1+\lambda_2} - \frac{\lambda_0}{\lambda_0+\lambda_1(1+\tau_0)} \\ &\quad + \frac{\lambda_0}{\lambda_1(1+\tau_0)+\lambda_0+\lambda_2}. \end{aligned} \quad (6)$$

Case 3 ($MC_1 > 0$, $MC_2 < 0$): In this case, it follows from Lemmas 1 and 2 that

$$\begin{aligned} &\lim_{P_s\to\infty} P_{out3}^{comm} \\ &= \frac{\lambda_0}{\lambda_0+\lambda_2} - \frac{\lambda_0}{\lambda_0+\lambda_1+\lambda_2} - \frac{\lambda_0}{\lambda_0+\lambda_2(1+\tau_0)} \\ &\quad + \frac{\lambda_0}{\lambda_0+\lambda_1+\lambda_2(1+\tau_0)}. \end{aligned} \quad (7)$$

Cases 4-1 and 4-2 ($MC_2 > 0$, $MC_1 > 0$): Under the scenario of $\gamma_{1c} < \gamma_{2c}$, BD1 will be scheduled as the transmitter such that a higher received SNR to decode the backscatter signal can be achieved at BD2. On the contrary, if $\gamma_{1c} > \gamma_{2c}$, BD2 will be scheduled as the backscatter transmitter. With the aid of Lemmas 1 and 2, when $P_s \to \infty$, it follows from Table II that probability of *Case 4* can be asymptotically expressed as

TABLE II
THE EXPRESSION OF P_{out4}^{comm}

CSI conditions	The corresponding expression of outage probability
$\gamma_{1c}<\gamma_{2c}$ $MC_1>0$ $MC_2>0$	$\Pr\left(1<\frac{X}{Z}<P_s\eta_2YU+1, 1<\frac{Y}{Z}<P_s\eta_1XU+1, X<Y, \frac{Y}{Z}-1<\tau_0\right)+\Pr\left(1<\frac{X}{Z}<P_s\eta_2YU+1, \frac{Y}{Z}>P_s\eta_1XU+1, \frac{X}{Z}<XUP_s\eta_1+1, P_s\eta_1XU<\tau_0\right)$ $+\Pr\left(1<\frac{Y}{Z}<P_s\eta_1XU+1, \frac{X}{Z}>P_s\eta_1YU+1, \frac{Y}{Z}>YUP_s\eta_2+1, \frac{Y}{Z}<\tau_0+1\right)+\Pr\left(\frac{X}{Z}>P_s\eta_2YU+1, \frac{Y}{Z}>P_s\eta_1XU+1, \frac{X}{Y}>\frac{\eta_2}{\eta_1}, P_s\eta_1XU<\tau_0\right)$
$\gamma_{1c}>\gamma_{2c}$ $MC_1>0$ $MC_2>0$	$\Pr\left(1<\frac{X}{Z}<P_s\eta_2YU+1, 1<\frac{Y}{Z}<P_s\eta_1XU+1, X>Y, \frac{X}{Z}-1<\tau_0\right)+\Pr\left(1<\frac{X}{Z}<P_s\eta_2YU+1, \frac{Y}{Z}>P_s\eta_1XU+1, \frac{X}{Z}>XUP_s\eta_1+1, \frac{X}{Z}<\tau_0+1\right)$ $+\Pr\left(1<\frac{Y}{Z}<P_s\eta_1XU+1, \frac{X}{Z}>P_s\eta_2YU+1, \frac{Y}{Z}<YUP_s\eta_2+1, P_s\eta_2YU<\tau_0\right)+\Pr\left(\frac{X}{Z}>P_s\eta_2YU+1, \frac{Y}{Z}>P_s\eta_1XU+1, \frac{X}{Y}<\frac{\eta_2}{\eta_1}, P_s\eta_2YU<\tau_0\right)$

$$\begin{aligned} &\lim_{P_s\to\infty} P_{out4}^{comm} \\ &= \frac{\lambda_0}{\lambda_0+\lambda_1+\lambda_2} + \frac{\lambda_0}{\lambda_0+(\lambda_1+\lambda_2)(1+\tau_0)} \\ &\quad - \frac{\lambda_0}{\lambda_0+\lambda_1+\lambda_2(1+\tau_0)} - \frac{\lambda_0}{\lambda_0+\lambda_1(1+\tau_0)+\lambda_2}. \end{aligned} \quad (8)$$

By summarizing the foregoing results, at high SNR, the outage probability can be asymptotically expressed as

$$\begin{aligned} &\lim_{P_s\to\infty} P_{out}^{comm} \\ &= \frac{\lambda_0}{\lambda_0+(\lambda_1+\lambda_2)(1+\tau_0)} - \frac{\lambda_0}{\lambda_0+\lambda_2(1+\tau_0)} \\ &\quad + 1 - \frac{\lambda_0}{\lambda_0+\lambda_1(1+\tau_0)}. \end{aligned} \quad (9)$$

Remark 1: It follows from (9) that at high SNR, the system outage probability becomes irrelevant to λ_{12}, η_1 and η_2. In particular, at high SNR, the outage performance of the backscatter link is not affected by the channel statistics of the backscatter link BD1-BD2, and it approaches to an error floor which is determined by the primary link PT-PR, decoding threshold τ_0 as well as two carrier transmission channels PT-BD1 and PT-BD2. To demonstrate the superiority of the proposed OppCom mechanism, we further consider the conventional fixed commensal (FibCom) mechanism, where one BD is fixedly designated as the transmitter, while the other BD serves as the receiver. According to Appendix B, at high SNR, the outage probability of the OppCom mechanism is always less than that of the FibCom mechanism.

B. OppPar Mechanism

For the OppPar mechanism, we set $\alpha = 1$ to boost the transmission robustness of the backscatter link. To guarantee the successful decoding of $C_2(n)$ (or $C_1(n)$) at the backscatter receiver, the following condition has to be satisfied: $\gamma_{1c} > \tau_0$ (i.e., $P_s\eta_2|h_2|^2|h_{12}|^2 > \tau_0$) or $\gamma_{2c} > \tau_0$ (i.e., $P_s\eta_1|h_1|^2|h_{12}|^2 > \tau_0$), respectively.

Case 1 ($P_1 < 0$,$P_2 < 0$):

$$P_{out1}^{paras} = \Pr(X < Z, Y < Z)$$

$$= 1 + \frac{\lambda_0}{\lambda_0+\lambda_1+\lambda_2} - \frac{\lambda_0}{\lambda_0+\lambda_1} - \frac{\lambda_0}{\lambda_0+\lambda_2}. \tag{10}$$

Case 2 ($P_1 < 0$, $P_2 > 0$): In this case, only BD2 can be selected as Tx. For such, the transmit power is set to $P_s = P_2$, and the transmission outage occurs when BD1 can not decode $C_2(n)$. Therefore, the outage probability in this case can be calculated as

$$\begin{aligned} P_{out2}^{paras} &= \Pr(X < Z, Z < Y < (1+\tau_0)Z) \\ &= \frac{\lambda_0}{\lambda_0+\lambda_1} - \frac{\lambda_0}{\lambda_0+(1+\tau_0)\lambda_1} - \frac{\lambda_0}{\lambda_0+\lambda_1+\lambda_2} \\ &\quad + \frac{\lambda_0}{\lambda_0+\lambda_2+(1+\tau_0)\lambda_1}. \end{aligned} \tag{11}$$

Case 3 ($P_1 > 0$, $P_2 < 0$): Based on symmetry between Cases 2 and 3, the outage probability of Case 3 can be readily attained as

$$\begin{aligned} P_{out3}^{paras} &= \frac{\lambda_0}{\lambda_0+\lambda_2} - \frac{\lambda_0}{\lambda_0+(1+\tau_0)\lambda_2} - \frac{\lambda_0}{\lambda_0+\lambda_1+\lambda_2} \\ &\quad + \frac{\lambda_0}{\lambda_0+\lambda_1+(1+\tau_0)\lambda_2}. \end{aligned} \tag{12}$$

Cases 4-1 and 4-2 ($P_1 > 0$, $P_2 > 0$): In these two cases, both BD1 and BD2 can decode $S(n)$. To enhance the transmission robustness of the backscatter link, we choose the node designation solution with the maximal SNR to decode $C_1(n)$ (or $C_2(n)$) at the backscatter receiver. If $\gamma_{1c} < \gamma_{2c}$, this inequality can be rewritten as $|h_2|^2/|h_1|^2 < \eta_1/\eta_2$. In this case, BD1 is selected as the backscatter transmitter. Otherwise, if $\gamma_{2c} < \gamma_{1c}$ ($|h_2|^2/|h_1|^2 > \eta_1/\eta_2$), BD2 is selected as the transmitter. For the case of $\gamma_{1c} < \gamma_{2c}$, the outage probability can be expressed as

$$P_{out4-1}^{paras} = \Pr\left(Z < Y < (1+\tau_0)Z, X > Z, Y < \frac{\eta_1}{\eta_2}X\right). \tag{13}$$

To proceed, we define $\eta = \eta_1/\eta_2$ and consider the following three cases, a.k.a., $\eta < 1$, $1 < \eta < 1+\tau_0$, and $\eta > 1+\tau_0$, such that (13) can be calculated as

$$P_{out4-1}^{paras} = \begin{cases} \dfrac{\tau_0\lambda_0\lambda_2}{(\lambda_0+\lambda_2+\frac{\lambda_1}{\eta})[\lambda_0+(\frac{\lambda_1}{\eta}+\lambda_2)(1+\tau_0)]}, \\ \qquad \eta < 1 \\ \dfrac{-\lambda_0[(1+\tau_0)\lambda_1+\eta\lambda_0+\eta^2\lambda_2]}{(\lambda_0+\lambda_1+\lambda_2\eta)[\lambda_0\eta+(\lambda_1+\lambda_2\eta)(1+\tau_0)]} \\ \quad + \dfrac{\lambda_0}{\lambda_0+\lambda_1+\lambda_2}, \quad 1 < \eta < 1+\tau_0 \\ \dfrac{\lambda_0}{\lambda_0+\lambda_1+\lambda_2} - \dfrac{\lambda_0}{\lambda_0+\lambda_1+(1+\tau_0)\lambda_2}. \\ \qquad \eta > 1+\tau_0. \end{cases} \tag{14}$$

The derivation procedure of *Case 4-2* ($P_1 > 0, P_2 > 0, \gamma_{2c} < \gamma_{1c}$), whose expression of outage probability is defined as P_{out4-2}^{paras}, is the same with P_{out4-1}^{paras}, is omitted here due to space limit. To summarize, we have $P_{out4}^{paras} = P_{out1}^{paras} + P_{out2}^{paras} + P_{out3}^{paras} + P_{out4-1}^{paras} + P_{out4-2}^{paras}$, which is shown in Table III.

TABLE III

THE OUTAGE PROBABILITY OF OPPPAR MECHANISM

The range of η	The expression of P_{out}^{paras}
$\eta < \frac{1}{1+\tau_0}$	$1 - \frac{\lambda_0}{\lambda_0+(1+\tau_0)\lambda_1} - \frac{\lambda_0}{\lambda_0+(1+\tau_0)\lambda_2} + \frac{\lambda_0}{\lambda_0+(1+\tau_0)\lambda_2+\lambda_1} + \frac{\tau_0\lambda_0\lambda_2}{(\lambda_0+\lambda_2+\frac{\lambda_1}{\eta})(\lambda_0+(1+\tau_0)(\lambda_2+\frac{\lambda_1}{\eta}))}$
$\frac{1}{1+\tau_0} < \eta < 1+\tau_0$	$1 - \frac{\lambda_0}{\lambda_0+(1+\tau_0)\lambda_1} - \frac{\lambda_0}{\lambda_0+(1+\tau_0)\lambda_2} + \frac{\lambda_0}{\lambda_0+(1+\tau_0)\lambda_2+\lambda_1} + \frac{\lambda_0}{\lambda_0+(1+\tau_0)\lambda_1+\lambda_2} + \frac{\tau_0\lambda_0\lambda_1}{(\lambda_0+\lambda_2\eta+\lambda_1)(\lambda_0+(\lambda_1+\lambda_2\eta)(1+\tau_0))} - \frac{\lambda_0[(1+\tau_0)\lambda_1+\eta\lambda_0+\eta^2\lambda_2]}{(\lambda_0+\lambda_1+\lambda_2\eta)[\lambda_0\eta+(\lambda_1+\lambda_2\eta)(1+\tau_0)]}$
$\eta > 1+\tau_0$	$1 - \frac{\lambda_0}{\lambda_0+(1+\tau_0)\lambda_1} - \frac{\lambda_0}{\lambda_0+(1+\tau_0)\lambda_2} + \frac{\lambda_0}{\lambda_0+(1+\tau_0)\lambda_1+\lambda_2} + \frac{\tau_0\lambda_0\lambda_1}{(\lambda_0+\lambda_1+\eta\lambda_2)(\lambda_0+(1+\tau_0)(\lambda_1+\eta\lambda_2))}$

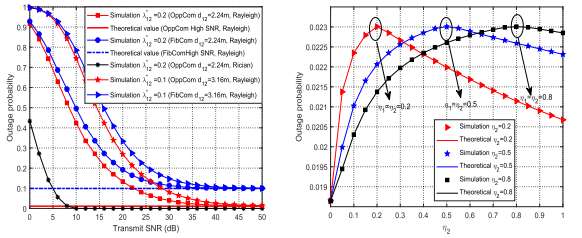

(a) (b)

Fig. 2. System outage probability of the OppCom and OppPar mechanisms. (a) System outage probability of the OppCom mechanism. (b) System outage probability of the OppPar mechanism.

Remark 2: It can be observed from Table III that the system outage probability is irrelevant to λ_{12}, which is similar to the OppCom mechanism. In addition, when $\eta_2/\eta_1 = 1$, the worst outage performance appears. At the same time, it can be found that for the OppPar mechanism, the outage probability is irrelevant to the specific values of η_1 and η_2, but only depends on the ratio between them. By following a similar procedure as in Appendix B, it can be proved that the outage probability of the OppPar mechanism is less than that of the FibPar mechanism.

IV. NUMERICAL RESULTS AND DISCUSSION

In this section, we adopt the well-known path loss model $\lambda^* = d^{-\beta}$, where d denotes the link distance and the path loss exponent β is set to 2.

Fig. 2 (a) shows the system outage probability of the OppCom mechanism under different λ_{12}^* ($\tau_0 = -5dB$, $\eta_1 = 1$, $\eta_2 = 1$, $\lambda_0^* = 0.01$, $\lambda_1^* = 0.2$, $\lambda_2^* = 0.1$). Based on Rician fading (LOS link) assumption, we simulate the outage performance with $\lambda_{12}^* = 0.2$ and a Rician K factor setup of $K = 10$. It can be first observed that the analytical results match well with simulations at high SNR. In addition, it follows from the figure that $P_{out}^{comm(fr)} - P_{out}^{comm} > 0$, which validates the superiority of the proposed OppCom mechanism over the FibCom mechanism, as predicted by *Remark 1*. Fig. 2 (b) corroborates our analysis for the OppPar mechanism and also shows that the worst outage performance of the OppPar mechanism appears when $\eta_2/\eta_1 = 1$ ($\lambda_0^* = 0.01$, $\lambda_1^* = 0.2$, $\lambda_2^* = 0.1$, $\lambda_{12}^* = 0.5$, $\tau_0 = 1dB$).

We take the OppCom mechanism as an example to show the advantage of our proposal over the non-spectrum sharing mechanism (benchmark 1) and the frequency-division

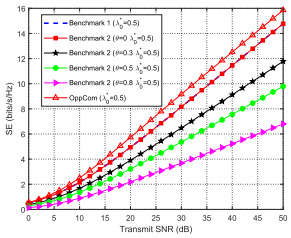

Fig. 3. The SE of benchmark 1, benchmark 2, and OppCom ($\tau_0 = 1$dB, $\lambda_1^* = \lambda_2^* = \lambda_{12}^* = 0.5$, $\eta_1 = \eta_2 = 1$).

multiplexing (FDM) based spectrum sharing mechanism (benchmark 2). For benchmark 1, the backscatter link is not present and the spectrum efficiency (SE) can be expressed as $\mathrm{SE}_{b1} = \mathrm{E}[\log_2(1 + P_s Z)]$. For benchmark 2, θ percentage of the bandwidth is allocated to the backscatter link, whereas $1-\theta$ percentage of the bandwidth is allocated to the primary link such that the SE of benchmark 2 is given by $\mathrm{SE}_{b2} = \theta\{\underset{\sigma_{b2,1b}}{\mathrm{E}}[\log_2(1 + P_s\eta_1 XU)] + \underset{\sigma_{b2,2b}}{\mathrm{E}}[\log_2(1 + P_s\eta_2 YU)]\} + (1-\theta)\mathrm{E}[\log_2(1 + P_s Z)]$, in which $\sigma_{b2,1b} = (Y > Z, Y > X, P_s\eta_1 XU > \tau_0)$ and $\sigma_{b2,2b} = (X > Z, X > Y, P_s\eta_2 YU > \tau_0)$. In addition, the SE of OppCom can be written as $\mathrm{SE}_{Com} = \underset{\sigma_{1b}}{\mathrm{E}}[\log_2(1+\gamma_{1c})] + \underset{\sigma_{2b}}{\mathrm{E}}[\log_2(1+\gamma_{2c})] + \mathrm{E}[\log_2(1 + P_s Z)]$, in which $\sigma_{1b} = (MC_1 < 0, MC_2 > 0, \gamma_{1c} > \tau_0) \cup (MC_1 > 0, MC_2 > 0, \gamma_{1c} > \gamma_{2c}, \gamma_{1c} > \tau_0)$ and $\sigma_{2b} = (MC_1 > 0, MC_2 < 0, \gamma_{2c} > \tau_0) \cup (MC_1 > 0, MC_2 > 0, \gamma_{2c} > \gamma_{1c}, \gamma_{2c} > \tau_0)$.

It follows from Fig. 3 that OppCom outperforms benchmarks 1 and 2 in terms of SE, which shows the advantage of the proposed symbiotic backscatter mechanism over the non-spectrum-sharing mechanism (benchmark 1) and the FDM-based spectrum-sharing mechanism (benchmark 2).

Appendix A

We assume that X, Y, and Z are independent random variables with arbitrary distributions. For sufficiently high transmit power P, it is ready to attain

$$\begin{aligned}\lim_{P\to\infty} &\Pr(X < PY, X < Z)\\ &= \lim_{P\to\infty} \int_0^{+\infty} (F_z(+\infty) - F_z(x))\\ &\quad \times (F_y(+\infty) - F_y(\frac{x}{P}))f_x(x)dx, \end{aligned} \tag{A.1}$$

where $f_*(*)$ and $F_*(*)$ denote the probability density function (PDF) and cumulative distribution function (CDF) of an arbitrary distribution, respectively.

Assume that we can find a M which satisfies to: $M \to +\infty$, but $\frac{M}{P} \to 0$, (A.1) can be asymptotically written as $\lim_{P\to\infty} \Pr(X < PY, X < Z) = Q_1 + Q_2$, where Q_1 and Q_2 can be respectively expressed as

$$\begin{aligned} Q_1 = &\lim_{P\to\infty M\to\infty} \int_0^{M} (F_z(+\infty) - F_z(x))(F_y(+\infty)\\ &- F_y(\frac{x}{P}))f_x(x)dx,\\ Q_2 = &\lim_{P\to\infty M\to\infty} \int_M^{+\infty} (F_z(+\infty) - F_z(x))(F_y(+\infty)\\ &- F_y(\frac{x}{P}))f_x(x)dx. \end{aligned} \tag{A.2}$$

As $P \to \infty$, it is ready to show that the integrand of Q_1 is Riemann integrable such that Q_1 can be written as

$$Q_1 = \int_0^{+\infty} (F_z(+\infty) - F_z(x))f_x(x)dx = \Pr(X < Z). \tag{A.3}$$

Since $0 < (F_z(+\infty) - F_z(x))(F_y(+\infty) - F_y(\frac{x}{P}))f_x(x) < f_x(x)$, one can arrive at

$$0 < Q_2 < \lim_{M\to+\infty} \int_M^{+\infty} f_x(x)dx = 0. \tag{A.4}$$

According to the Squeeze Theorem, we have $Q_2 = 0$, which by its turn leads to

$$\lim_{P\to\infty} \Pr(X < PY, X < Z) = \Pr(X < Z). \tag{A.5}$$

Appendix B

Assume BD1 as transmitter and BD2 as receiver, the probability that BD2 cannot decode $S(n)$ can be written as

$$P_{out1}^{comm(fr)} = \Pr(Y < Z). \tag{B.1}$$

If BD2 successfully decodes $S(n)$ but it cannot decode $C_1(n)$, we have

$$P_{out2}^{comm(fr)} = \Pr(Y > Z, P_s\alpha_1\eta_1 XU < \tau_0). \tag{B.2}$$

With the aid of Lemmas 1 and 2, when $P_s \to +\infty$, $P_{out}^{comm(fr)}$ can be expressed as

$$\lim_{P_s\to+\infty} P_{out}^{comm(fr)} = 1 - \frac{\lambda_0}{\lambda_0 + \lambda_2(1+\tau_0)}. \tag{B.3}$$

References

[1] J. Lin, W. Yu, N. Zhang, X. Yang, H. Zhang, and W. Zhao, "A survey on Internet of Things: Architecture, enabling technologies, security and privacy, and applications," *IEEE Internet Things J.*, vol. 4, no. 5, pp. 1125–1142, Oct. 2017.

[2] I. Lee and K. Lee, "The Internet of Things (IoT): Applications, investments, and challenges for enterprises," *Bus. Horizons*, vol. 58, no. 4, pp. 431–440, 2015.

[3] V. Liu, A. Parks, V. Talla, S. Gollakota, D. Wetherall, and J. R. Smith, "Ambient backscatter: Wireless communication out of thin air," *ACM SIGCOMM Comput. Commun. Rev.*, vol. 43, no. 4, pp. 39–50, Aug. 2013.

[4] N. Van Huynh, D. T. Hoang, X. Lu, D. Niyato, P. Wang, and D. I. Kim, "Ambient backscatter communications: A contemporary survey," *IEEE Commun. Surveys Tuts.*, vol. 20, no. 4, pp. 2889–2922, 4th Quart., 2018.

[5] L. Zhang, Y.-C. Liang, and M. Xiao, "Spectrum sharing for Internet of Things: A survey," *IEEE Wireless Commun.*, vol. 26, no. 3, pp. 132–139, Jun. 2019.

[6] H. Guo, Y.-C. Liang, R. Long, and Q. Zhang, "Cooperative ambient backscatter system: A symbiotic radio paradigm for passive IoT," *IEEE Wireless Commun. Lett.*, vol. 8, no. 4, pp. 1191–1194, Aug. 2019.

[7] H. Ding, D. B. da Costa, and J. Ge, "Outage analysis for cooperative ambient backscatter systems," *IEEE Wireless Commun. Lett.*, vol. 9, no. 5, pp. 601–605, May 2020.

[8] A. Bentrcia, A. U. Sheikh, and A. Zerguine, "A new ordering and grouping algorithm for the linear weighted group matched filter successive interference cancellation detector," *IEEE Trans. Veh. Technol.*, vol. 55, no. 2, pp. 704–709, Mar. 2006.

[9] T. Eltaif, H. M. H. Shalaby, and S. Shaari, "A novel successive interference cancellation scheme in OCDMA system," in *Proc. IEEE Int. Conf. Semicond. Electron.*, Nov. 2006, pp. 299–303.

[10] Y. Ye, L. Shi, X. Chu, and G. Lu, "On the outage performance of ambient backscatter communications," *IEEE Internet Things J.*, vol. 7, no. 8, pp. 7265–7278, Aug. 2020.

[11] I. S. Gradshteyn and I. M. Ryzhik, *Table of Integrals, Series, and Products*. New York, NY, USA: Academic, 2014.